Electrochemical Capacitors with High Output Voltages that Mimic Electric Eels

*Hao Sun, Xuemei Fu, Songlin Xie, Yishu Jiang, and Huisheng Peng**

Nature is a source of inspiration for advancing science and technology.[1–5] Although bioinspired materials have been intensively explored for various functionalities, however, to imitate and create more complex and tunable electronic devices from biological structures is rare. Electric eels, the strongest bioelectricity producer in the animal kingdom, can generate high voltage discharges to stun prey and ward off predators.[6–10] Considerable effort has been made to understand electricity generation from electrocytes on the cellular and genetic level.[6,7,10] Although any single electrocyte in the electric eel only produces a low voltage of ≈0.15 V, a regular in-series arrangement of thousands of electrocytes produces high voltages of up to 600 V (**Figure 1**). This unique organization has inspired humans to develop functional materials for decades. However, such a natural strategy has never been used to fabricate high-performance electronic devices. Furthermore, accurately controlling efficient connection when fabricating complex yet tunable electronic devices is essential and remains a challenge to the advancement of microelectronics. Taking the electrochemical capacitor as an example, water-based electrolytes are favored over their organic-based counterparts due to safety concerns for wearable applications.[11–14] However, the maximal working voltages are limited by the thermodynamic decomposition potential of water (≈1.23 V), which barely meets the voltage requirements for a variety of electronic devices or products. Traditional assemblies with external conducting wires suffer from many disadvantages, including complex preparation processes and high costs; both safety and the level of integration are also sacrificed, particularly when connecting a large number of power devices. To this end, simple and effective strategies for integrating electrochemical capacitors are desired but currently unavailable.

Herein, a new family of flexible electrochemical capacitors has been developed by mimicking the in-series structure for electrocytes in the electric eel to produce high working voltages. These structures possess a unique fiber shape and are flexible, stretchable, and weavable, which is particularly promising for portable and wearable electronics. In addition, the electrochemical capacitors can be further integrated with solar cells to realize high-performance self-powered systems with high output voltages incorporating the in-series structure.

The fabrication of in-series fibrous electrochemical capacitors is schematically demonstrated in **Figure 2**a–c. An elastic fiber with a diameter of 500 μm served as a stretchable substrate to make the resulting electrochemical capacitors stretchable. Aligned multiwalled carbon nanotube (MWCNT) sheets spun from a MWCNT array were continuously wrapped onto the elastic fiber surface with an intersectional angle of 60°. MWCNT sheets with a length of 0.2 cm were wiped off at certain intervals by removing the paper covering the fibers before wrapping with the MWCNT sheet (Figure 2a) and followed by coating poly(vinyl alcohol)/H_3PO_4 gel electrolyte (Figure 2b). The middle of each MWCNT segment was left without an electrolyte coating to act as a common electrode. The four rectangles in Figure 2b indicate the four electrochemical capacitor units in an in-series connection. These in-series fiber-shaped devices were highly flexible and stretchable (Figure 2c), and shared a uniform diameter (Figure 2d).

Gel electrolyte plays an important role in energy storage. The dependence of the electrochemical performance on the coating method, gel viscosity, and coating thickness was investigated. Both spray and brush coating methods were available for the current system. For the spray coating, a uniform layer can be achieved at a viscosity below 0.32 Pa s^{-1}, and the airbrush would be blocked beyond this point. In contrast, a brush coating produced uniform layers at viscosities ranged from 0.03 to 2.27 Pa s^{-1}. The specific capacitances were slightly fluctuated around 11 F g^{-1} below 0.32 Pa s^{-1} and decreased to 6.0 F g^{-1} at 2.27 Pa s^{-1} (Figure S1, Supporting Information). The permeating resistances of gel electrolyte into MWCNT sheets were decreased with decreasing viscosities, which increased the specific capacitances. However, the film-forming properties of the electrolyte were poor at low viscosities, resulting in a deficient contact with MWCNT sheets. Therefore, the decreased degree in specific capacitance was lower at lower viscosities compared with the cases at higher viscosities. Similar specific capacitances had been achieved for the above two methods under the same condition (Figure S2, Supporting Information). Here, a viscosity of 0.32 Pa s^{-1} was mainly used for the brush coating method. Note that the spray coating employed a lower viscosity of 0.10 Pa s^{-1} for a good performance. The coating thicknesses can be controlled by varying the spraying duration. The specific capacitances had been increased with increasing thicknesses from ≈2.5 to 15 μm due to better coverage of electrolyte (Figure S3a, Supporting Information) and then reached a platform at higher thicknesses (Figure S4, Supporting Information).

The aligned structure of the MWCNT sheets on the elastic fiber was clearly observed via scanning electron microscopy (SEM) and was beneficial for rapid electron transport along the length of the MWCNT (Figures 2e,f). The close contact between the aligned MWCNT and elastic fiber substrate, which was important for flexible, high-performance applications, was verified by SEM (Figures 2g,h). Importantly, the gel electrolyte was effectively penetrated into the aligned MWCNTs

H. Sun, X. Fu, S. Xie, Y. Jiang, Prof. H. Peng
State Key Laboratory of Molecular Engineering of Polymers
Department of Macromolecular Science and Laboratory of Advanced Materials
Fudan University
Shanghai 200438, China
E-mail: penghs@fudan.edu.cn

DOI: 10.1002/adma.201505742

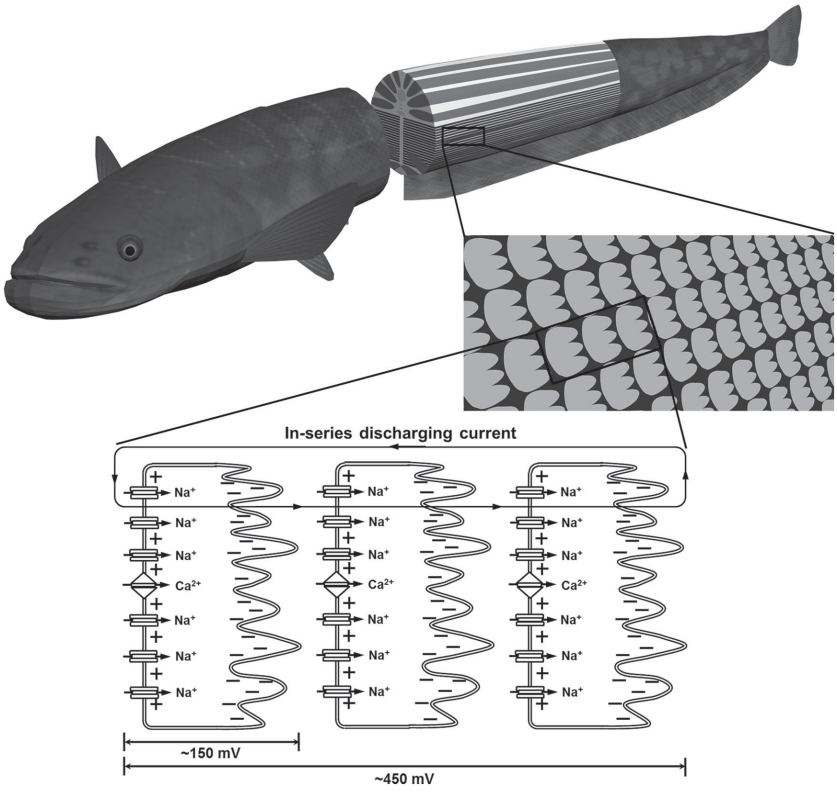

Figure 1. Schematic of the in-series electrocyte arrangement in an electric eel.

(Figure S5, Supporting Information). In addition, the MWCNT alignment was maintained after coating with the gel electrolyte (Figures 2i,j). The electrodes were extracted from the common electrodes, and the maximal working voltages were controlled by varying the unit number between the two extracting electrodes.

The capacitive performance of one electrochemical capacitor unit was investigated. The galvanostatic charge–discharge curves for electrochemical capacitors with 0.5, 1, 1.5, and 2.5 cm long electrodes were obtained under similar conditions (Figure S6, Supporting Information). The discharge time increased linearly from 10.3 to 59.6 s when increasing the length from 0.5 to 2.5 cm. The energy storage performance could be controlled by varying the amount of electrode material, i.e., the MWCNT sheet thickness. The discharge time increased from 10.3 to 77.5 s upon increasing the MWCNT thickness from 0.32 to 1.92 μm (Figure S7, Supporting Information). Herein, electrochemical capacitors with 0.5 cm long electrodes and 0.32 μm thick MWCNT sheets were used unless specified otherwise.

The galvanostatic charge–discharge curves all shared a symmetrical triangle shape for increasing current densities from 0.12 to 1.00 A g^{-1} with high coulombic efficiencies fluctuating around 96%, which indicated a high reversibility during the charge–discharge process (Figure S8a, Supporting Information). The cyclic voltammograms exhibited typical rectangular shapes of a double-layer electrochemical capacitor. These rectangular shapes were retained upon increasing the scan rates from 50 to 500 mV s^{-1}, which indicates high electrochemical stability (Figure S8b, Supporting Information). The specific capacitance reached 11.72 F g^{-1} with a current density of 0.06 A g^{-1}. The electrochemical performance can be further improved by incorporating other pseudocapacitive materials. For instance, polyaniline (PANI) was deposited onto the MWCNTs via electropolymerization to increase the specific capacitance (Figure S9, Supporting Information). The PANI weight can be controlled by varying the charge during the electrochemical polymerization. The specific capacitances increased from 9.92 to 213.12 F g^{-1} after increasing the weight percentage from 0 to 70% and decreased after increasing the weight percentage further, e.g., 107.53 F g^{-1} at 80% (Figure S10, Supporting Information). The electrochemical capacitor exhibited high charge–discharge stability under increasing current densities, even at a high PANI weight percentage of 70 wt% (Figure S11, Supporting Information).

The maximal working voltage can be readily increased by increasing the unit number. As a demonstration, the galvanostatic charge–discharge curves for in-series fiber-shaped electrochemical capacitors containing five and ten electrochemical capacitor units were investigated, and the highest working voltages reached 5 and 10 V, respectively (Figure S12, Supporting Information). The triangle shapes were maintained even at a working voltage of 10 V with coulombic efficiencies ranged from 72.6% to 97.3% (Figure S12b, Supporting Information), which were comparable to ≈45% to 100% for the reported flexible electrochemical capacitors without metal current collectors.[15,16] One concern lies in the possible migration of gel electrolyte among neighboring units driven by the capillary force of aligned MWCNTs, which may form ionic channels and lose the electrochemical capability for the in-series connection. Fortunately, the above phenomenon did not occur even for the gel electrolyte with the lowest viscosity of 0.03 Pa s^{-1} (Figure S13, Supporting Information). This may be explained by the hydrophobic nature of MWCNTs that hinders the migration of aqueous electrolyte along MWCNTs, particularly for a highly viscous gel electrolyte. The equivalent series resistances demonstrated a linear increase with the increasing unit number for a single unit of ≈8 kΩ at the MWCNT thickness of 3.84 μm (Figure S14a, Supporting Information). The incorporation of PANI was beneficial for the reduction of the equivalent series resistance, e.g., ≈1.7 kΩ for a single unit at the same MWCNT thickness (Figure S14b, Supporting Information). It may be attributed to the enhanced contact among MWNCT bundles that reduced the electrical resistances based on a 3D hopping mechanism.[17] PANI with an enhanced hydrophily also contributed to the reduction of the interfacial resistance between the electrode material and electrolyte. The resulting equivalent series resistances were comparable to the reported flexible electrochemical capacitors without metal current collectors (Table S1, Supporting Information).[15,16] The linear increase in voltage with the number of electrochemical capacitor units was maintained after incorporating PANI, e.g., a voltage of 10 V was achieved

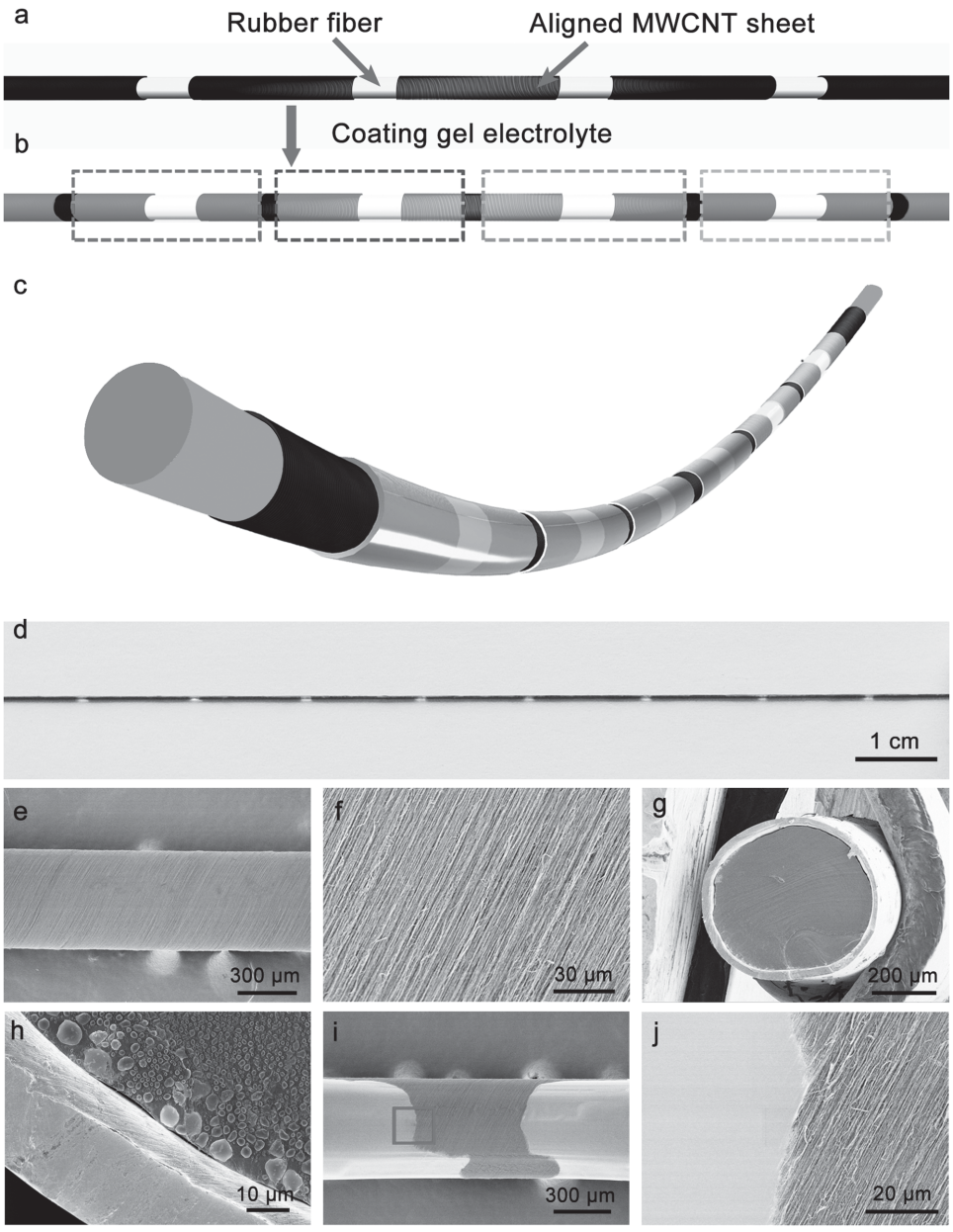

Figure 2. a–c) Schematic of the fabrication for an in-series fiber-shaped electrochemical capacitor. d) Photograph of an in-series fiber-shaped electrochemical capacitor containing eight units. e,f) SEM images of the aligned MWCNT sheet on the elastic fiber surface at low and high magnifications, respectively. g,h) Cross-sectional SEM images of the aligned MWCNT sheet wrapped elastic fiber coated with a gel electrolyte at low and high magnifications, respectively. i) SEM image of the interface between the aligned MWCNT sheet and gel electrolyte. j) Higher magnification of the rectangle area in panel (i).

for a fiber-shaped electrochemical capacitor containing ten units with 70 wt% PANI (Figure S15, Supporting Information). The charge–discharge current and capacitance can be enhanced by increasing the loading amounts of active materials. By increasing the total loading mass of active material from 0.04 to 0.24 mg cm^{-1}, the capacitances of five in-series units had been increased from 0.24 to 2.48 mF, and the maximal capacitance of a single unit reached 12.6 mF (Figures S16 and S17, Supporting Information). An electrochemical capacitor fiber with five in-series units with the active material of 0.24 mg cm^{-1} produced a high current of 200 μA (Figure S18, Supporting Information). As a result, the specific capacitances of one unit and five units based on the total mass of the device were calculated to be 485 and 95 mF g^{-1}, respectively, which can also be enhanced by reducing the diameter and density of the elastic fiber substrate.

High working voltages are required for a variety of applications. Using continuous fabrication technology, fiber-shaped electrochemical capacitors with 100, 200, 300, 400, 500, 600, 700, 800, 900, and 1000 units were fabricated and charged at a current density of 1.50 A g^{-1}. The maximal working voltages increased linearly with an increasing number of units and reached the values calculated for the unit number (**Figure 3**a,b).

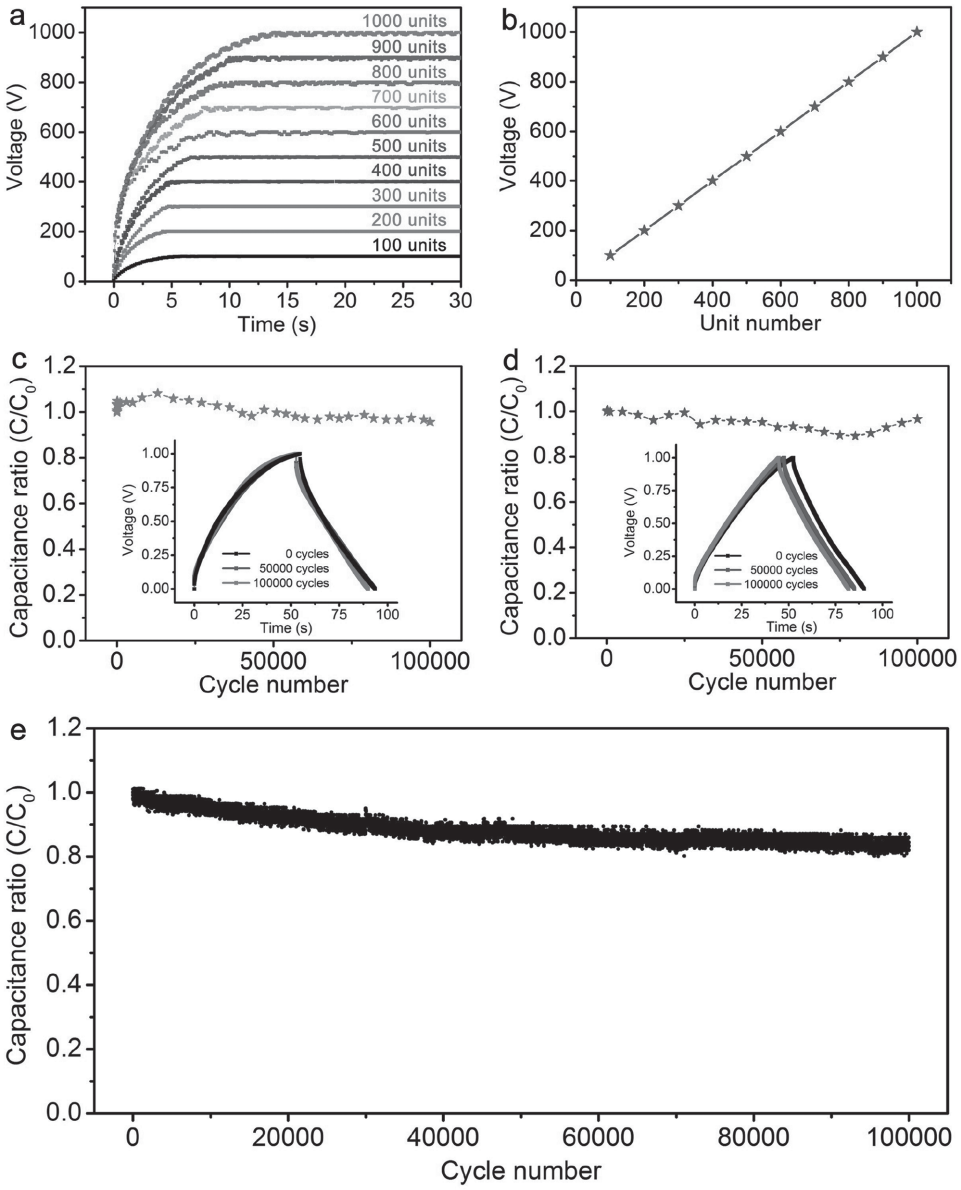

Figure 3. a) Dependence of the voltage on charging time for fiber-shaped electrochemical capacitors containing 100, 200, 300, 400, 500, 600, 700, 800, 900, and 1000 units connected in-series. The charging current density was 1.50 A g^{-1} for an electrochemical capacitor unit. b) Dependence of the maximal output voltage on the unit number. c) Capacitance variation for an electrochemical capacitor during 100 000 stretch cycles at a 50% strain. The inserted image represents the galvanostatic charge–discharge curves with different stretching cycles. d) Capacitance variation for an electrochemical capacitor over 100 000 bending cycles with a 1 cm radius of curvature. The inserted image represents the galvanostatic charge–discharge curves for different bending cycles. e) Capacitance variation for an electrochemical capacitor containing five in-series units over 100 000 galvanostatic charge–discharge cycles. The maximal voltage, 5 V. The current density for one electrochemical capacitor unit, 2.00 A g^{-1}.

A 1000 V output voltage was produced from an ≈12 m long fiber-shaped supercapacitor. These electronic devices could be made with electrode sizes below 50 nm via well-developed lithographic techniques,[18–21] and the maximal output voltage for the in-series fiber-shaped electrochemical capacitor was calculated as 6.7×10^6 V m^{-1}.

Apart from the high working voltage favoring practical applications, the fiber-shaped electrochemical capacitors were also stretchable and flexible. The compact contact between the electrode and gel electrolyte allows the as-fabricated in-series electrochemical capacitors to tolerate a maximal strain of up to 70% without structural damage or sacrificing the capacitance (Figures S19 and S20, Supporting Information). The specific discharge capacitance increased 38% at a strain of 70%, which may be attributed to the improved contact between the electrolyte and MWCNT at higher strains (Figure S20, Supporting Information). After stretching at a strain of 50% for 100 000 cycles, the specific capacitance was maintained at 95.6% (Figure 3c). The fiber-shaped electrochemical capacitor was intertwined onto various substrates (Figure S21, Supporting Information), and

its flexibility was verified from the galvanostatic charge–discharge results under bending with increasing curvatures. The electrochemical performance was well maintained when an ≈15 cm long fiber-shaped electrochemical capacitor was bent at a small radius of 0.3 cm (Figure S22, Supporting Information). The capacitance was maintained at 96.6% after bending for 100 000 cycles when a 4 cm long device was bent at a radius of curvature of 0.8 cm (Figure 3d). In addition, the capacitance for an electrochemical capacitor containing five in-series units remained 83.3% after 100 000 galvanostatic charge–discharge cycles (Figure 3e).

Ten in-series fiber-shaped electrochemical capacitors were woven with commercial elastic fibers to produce an energy textile that could be integrated into clothes (**Figure 4**a–c). These energy textiles can be fabricated with tunable working voltages and capacitances to power various miniature electronic devices. For instance, four in-series electrochemical capacitor fibers (each containing six units) were connected in parallel to form an "energy wristband" to support an electronic watch (Figure 4d). After charging with 10 μA current to 6 V, the "energy wristband" was connected to continuously power the electronic watch (Figure 4e). The flexible nature of the "energy wristband" also promised integration with the watch and served as a flexible and portable energy source (Figure 4f). Eighteen fiber-shaped electrochemical capacitors were divided into three parallel groups (dashed boxes in Figure 4g) with each group containing 120 in-series units, and woven into a T-shirt. After charging with 20 μA to 120 V, they can discharge to power 57 light-emitting diodes integrated into the T-shirt (Figure 4h).

The novel in-series design also made these energy fibers competitive compared with standard flexible electrochemical capacitor and conventional dielectric capacitor system such as the X7R variety. Compared with the former, the in-series electrochemical capacitor fiber demonstrated enhanced output voltage and integration level, and the stretchable and wearable features made them particularly promising for portable electronics and smart garment applications. As a kind of dielectric capacitor storing energy in the form of an electrostatic field between highly conductive electrodes, the X7R variety demonstrated a much lower equivalent series resistance (<0.1 Ω) that favored high-frequency circuit applications for blocking direct current, coupling and discriminating frequency (Table S1, Supporting Information). Here, the electrochemical capacitor fibers demonstrated much higher capacitances that enabled energy storage applications at low frequencies. In addition, the high flexibility, stretchability, and wearability well met the mainstream

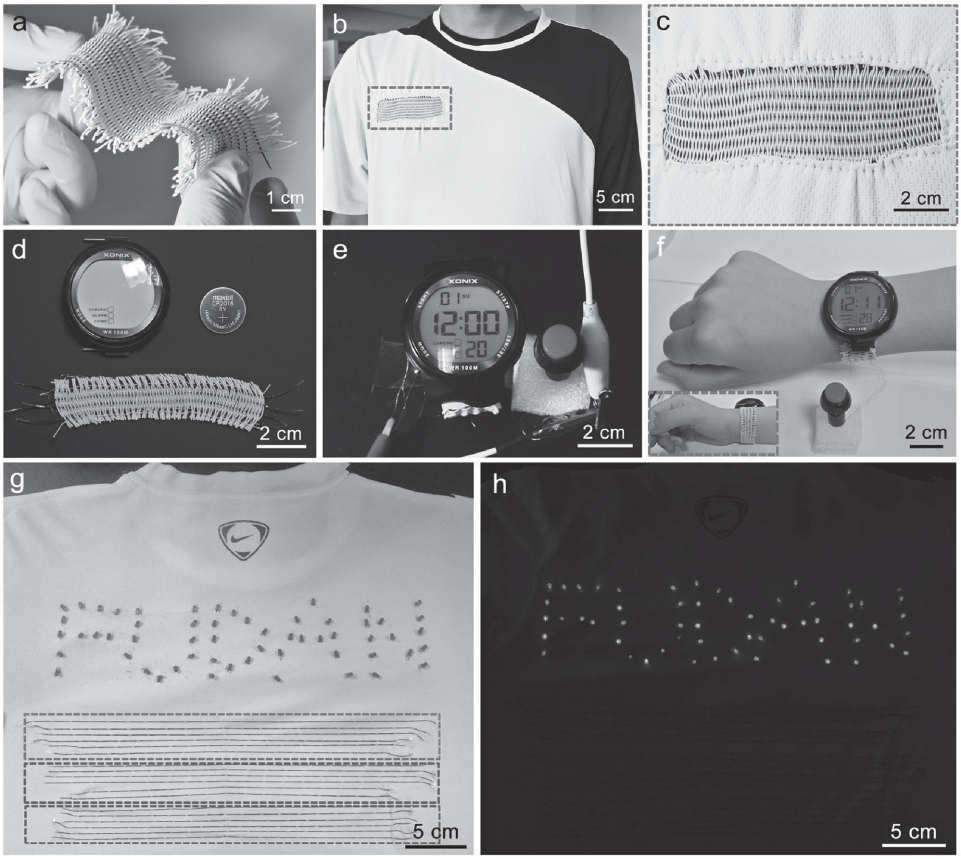

Figure 4. a–c) Energy textile composed of fiber-shaped electrochemical capacitors woven into a T-shirt. c) Amplification of the rectangle in panel (b). d–f) Energy textile woven from in-series electrochemical capacitor fibers used to power a commercial electronic watch. Each fiber-shaped electrochemical capacitor contained six units connected in series. The inserted image from panel (f) shows a side view of the electronic watch and energy textile. g,h) Eighteen fiber-shaped electrochemical capacitors divided into three in-parallel groups (the dashed boxes) and integrated into a T-shirt to power 57 red light-emitting diodes.

development of flexible electronics, which can hardly be met by the conventional rigid and blocky energy storage systems (Table S1, Supporting Information).

Based on a similar strategy, fiber-shaped solar cells were integrated with these electrochemical capacitors to realize both energy conversion and storage in one device. An in-series fiber-shaped energy-harvesting portion was first produced from a spring-like photoanode with dye-sensitized TiO_2 nanotube arrays grown on titanium wire and aligned MWCNT/elastic fiber as the counter electrode (Figure S23, Supporting Information). The aligned TiO_2 nanotubes and MWCNTs were beneficial for dye absorption, charge collection, and transport. A single unit offered a power conversion efficiency of 6.2% (Figure S24, Supporting Information). The in-series connection was realized by connecting the titanium wire from one part with aligned MWCNTs from a neighboring part before coating a thin layer of silver paste at the joint to reduce the contact resistance.

First, the photovoltaic performance for the energy-harvesting part was investigated. Increasing the number of units from 2 to 16 enhanced the power conversion efficiency with increasing open-circuit voltages from 1.26 to 9.98 V with short circuit currents and fill factors at 170 μA and 0.50, respectively (Figure S25, Supporting Information). The photogenerated voltage, 10 V, was sufficiently high to power typical electronic devices, and the in-series connection without any conducting wires improved the integration for the entire system considerably. The in-series fiber-shaped energy-harvesting and storage device was developed further by integrating the energy-harvesting portion (e.g., 16 units) and electrochemical capacitor (ten units) into one fiber using the aligned MWCNT sheet as a common electrode (Figure S26, Supporting Information). Under illumination, the energy harvesting portion charged the energy storage part (i.e., electrochemical capacitor) with a voltage rapidly exceeding 9.5 V (Figure S27, Supporting Information). During the discharge process, the energy storage portion could power other electronic facilities with various discharging current densities (Figure S27, Supporting Information).

In summary, a new family of in-series fiber-shaped electrochemical capacitors has been created to offer high output voltages up to 1000 V, the highest voltage among the energy storage devices to date. The structure design for an in-series connection prevents the use of a lot of conventional conducting wires with high efficiency. These in-series fiber-shaped electrochemical capacitors are flexible, stretchable, and weavable with high stability, and can be further integrated with solar cells to realize high-performance self-powered systems with high output voltages incorporating the in-series structure.

Experimental Section

Fabrication of the In-Series Fiber-Shaped Electrochemical Capacitor: A rubber fiber (500 μm in diameter) was used as the elastic substrate. Aligned MWCNT sheets were drawn out of a spinnable MWCNT array synthesized via chemical vapor deposition and continuously wrapped around the rubber fiber.[22] Gel electrolytes with increasing viscosities of 0.03, 0.10, 0.32, 0.50, and 2.27 Pa s^{-1} were prepared by dissolving 0.5, 0.75, 1.0, 1.2, and 1.4 g of poly(vinyl alcohol) (PVA1799, molecular weight of 74500, Aladdin) in 9 mL of deionized water and 1 g of H_3PO_4, respectively. The ionic conductivities were measured to be 63.7, 61.9, 61.3, 59.2, and 54.3 mS cm^{-1}, respectively. The MWCNT sheet in the middle without an electrolyte coating served as the common electrodes. Each electrochemical capacitor unit contained two MWCNT segments with a gel electrolyte on their surface. Spray and brush coating methods were performed to coat gel electrolytes onto MWCNTs. The fiber-shaped device was first fixed at two motors by two ends with a flexible polyethylene mask covering the common electrode, and the two motors were simultaneously rotated at the same rotation speed of ≈200 rpm. For the spray coating, an airbrush (HD-130, Holder) with the nozzle diameter of 0.5 mm was used with an inlet pressure of ≈1.5 bar and working distance of ≈5 cm. For the brush coating, gel electrolyte was dipped with a thin and soft writing brush and coated onto the rotated device. Different electrolyte thicknesses were obtained by varying the spraying durations using gel electrolyte at a viscosity of 0.03 Pa s^{-1}. The vacuum treatment was performed to enhance the permeation of gel electrolyte into electrode materials. Two common electrodes were extracted with copper wires, and the working voltages were controlled by varying their distance to tune the unit number. PANI was incorporated into the aligned MWCNTs via an electropolymerization method using 0.1 M aniline and 1.0 M H_2SO_4 as the electrolyte at 0.75 V versus saturated calomel electrode. The PANI mass was calculated assuming an average 2.5 electrons per aniline monomer.[23]

Fabrication of the In-Series Fiber-Shaped Integrated Device: A Ti wire (127 μm in diameter) was wound on a rigid steel substrate (600 μm in diameter) to form a spring before successively washing with acetone, isopropyl alcohol, and water. An anodic oxidation method was used to perpendicularly grow TiO_2 nanotube arrays on the Ti wire surface, followed by heating to 500 °C for 1 h and annealing in air. The resultant wire was immersed into an aqueous solution containing 40×10^{-3} M $TiCl_4$ at 70 °C for 0.5 h and annealing at 450 °C for 0.5 h. The modified Ti wire then adsorbed the dye N719 and was inserted with a MWCNT fiber counter electrode before injecting a redox electrolyte (containing 0.1 M lithium iodide, 0.05 M iodine, 0.6 M 1,2-dimethyl-3-propylimidazolium iodide, and 0.5 M 4-*tert* butyl-pyridine in dehydrated acetonitrile). This energy-harvesting portion was integrated with an electrochemical capacitor in series by sharing the elastic fiber and aligned MWCNT sheet electrodes (Figure S16, Supporting Information). The specific mass capacitance (C_m) was calculated from the equation $C_m = 2 \times I \times \Delta t/(\Delta V \times m)$, where I, Δt, ΔV, and m correspond to the discharge current, discharge time, voltage variation, and active material mass on one electrode, respectively. The capacitance (C) was calculated from the equation of $C = I \times \Delta t/\Delta V$. The specific capacitance (C_d) was calculated from the equation of $C_d = C/m_d$, where m_d is the total mass of the device.

Supporting Information

Supporting Information is available from the Wiley Online Library or from the author.

Acknowledgements

This work was supported by NSFC (21225417), MOST (2011CB932503), STCSM (12nm0503200), Fok Ying Tong Education Foundation, the Program for Professor of Special Appointment at Shanghai Institutions of Higher Learning, and the Program for Outstanding Young Scholars from Organization Department of the CPC Central Committee.

Received: November 19, 2015
Revised: December 3, 2015
Published online: January 14, 2016

[1] N. Savage, *Nature* **2015**, *519*, S7.
[2] Y. Zheng, H. Bai, Z. Huang, X. Tian, F.-Q. Nie, Y. Zhao, J. Zhai, L. Jiang, *Nature* **2010**, *463*, 640.

[3] Y. M. Song, Y. Xie, V. Malyarchuk, J. Xiao, I. Jung, K. J. Choi, Z. Liu, H. Park, C. Lu, R. H. Kim, *Nature* **2013**, *497*, 95.
[4] J. Gould, *Nature* **2015**, *519*, S2.
[5] K. Y. Ma, P. Chirarattananon, S. B. Fuller, R. J. Wood, *Science* **2013**, *340*, 603.
[6] M. Noda, S. Shimizu, T. Tanabe, T. Takai, T. Kayano, T. Ikeda, H. Takahashi, H. Nakayama, Y. Kanaoka, N. Minamino, *Nature* **1984**, *312*, 121.
[7] A. L. Gotter, M. A. Kaetzel, J. R. Dedman, *Comp. Biochem. Phys. A* **1998**, *119*, 225.
[8] X. U. Jian, D. A. Lavan, *Nat. Nanotechnol.* **2008**, *3*, 666.
[9] K. Catania, *Science* **2014**, *346*, 1231.
[10] J. R. Gallant, L. L. Traeger, J. D. Volkening, H. Moffett, P. H. Chen, C. D. Novina, G. N. Phillips, R. Anand, G. B. Wells, M. Pinch, *Science* **2014**, *344*, 1522.
[11] a) D. Yu, K. Goh, H. Wang, L. Wei, W. Jiang, Q. Zhang, L. Dai, Y. Chen, *Nat. Nanotechnol.* **2014**, *9*, 555; b) D. Yu, K. Goh, Q. Zhang, L. Wei, H. Wang, W. Jiang, Y. Chen, *Adv. Mater.* **2014**, *26*, 6790.
[12] a) Q. Meng, H. Wu, Y. Meng, K. Xie, Z. Wei, Z. Guo, *Adv. Mater.* **2014**, *26*, 4100; b) K. Wang, Q. Meng, Y. Zhang, Z. Wei, M. Miao, *Adv. Mater.* **2013**, *25*, 1494.
[13] a) L. Kou, T. Huang, B. Zheng, Y. Han, X. Zhao, K. Gopalsamy, H. Sun, C. Gao, *Nat. Commun.* **2014**, *5*, 3754; b) B. Zheng, T. Huang, L. Kou, X. Zhao, K. Gopalsamy, C. Gao, *J. Mater. Chem. A* **2014**, *2*, 9736.
[14] H. Sun, X. You, J. Deng, X. Chen, Z. Yang, J. Ren, H. Peng, *Adv. Mater.* **2014**, *26*, 2868.
[15] P. Xu, J. Kang, J. Choi, J. Suhr, J. Yu, F. Li, J. Byun, B. Kim, T. Chou, *ACS Nano* **2014**, *8*, 9437.
[16] P. Chen, H. Chen, J. Qiu, C. Zhou, *Nano Res.* **2010**, *3*, 594.
[17] H. Peng, M. Jain, D. E. Peterson, Y. Zhu, Q. Jia, *Small* **2008**, *4*, 1964.
[18] W. Shim, A. B. Braunschweig, X. Liao, J. Chai, J. K. Lim, G. Zheng, C. A. Mirkin, *Nature* **2011**, *469*, 516.
[19] L. Demers, D. Ginger, S.-J. Park, Z. Li, S.-W. Chung, C. Mirkin, *Science* **2002**, *296*, 1836.
[20] S. O. Kim, H. H. Solak, M. P. Stoykovich, N. J. Ferrier, J. J. de Pablo, P. F. Nealey, *Nature* **2003**, *424*, 411.
[21] M. P. Stoykovich, M. Müller, S. O. Kim, H. H. Solak, E. W. Edwards, J. J. De Pablo, P. F. Nealey, *Science* **2005**, *308*, 1442.
[22] Z. Yang, J. Deng, X. Chen, J. Ren, H. Peng, *Angew. Chem., Int. Ed.* **2013**, *52*, 13453.
[23] A. Yu, I. Roes, A. Davies, Z. Chen, *Appl. Phys. Lett.* **2010**, *96*, 253105.